JOC Articles

Conjugated Thiophene-Containing Oligoacenes Through Photocyclization: Bent Acenedithiophenes and a Thiahelicene

Agostino Pietrangelo, Brian O. Patrick, Mark J. MacLachlan,* and Michael O. Wolf*

Department of Chemistry, University of British Columbia, Vancouver, BC, Canada V6T 1Z1

mmaclach@chem.ubc.ca; mwolf@chem.ubc.ca

Received March 18, 2009

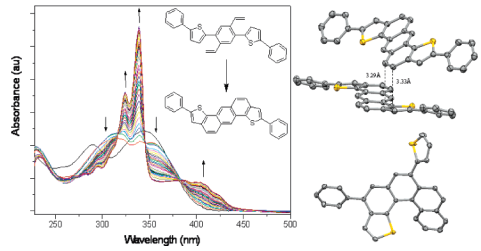

The preparation of bent anthradithiophenes (BADTs) using an oxidative photocyclization-based synthetic strategy is reported. The optical properties of the new compounds were characterized by UV−vis and fluorescence spectroscopies, and the redox properties were probed by cyclic voltammetry. Structural studies using single crystal X-ray crystallography show that the unsubstituted BADT adopts a slipped cofacial stacking arrangement in the solid state with $\pi-\pi$ interactions along the intermolecular stacking axis. The dialkylated derivatives adopt similar packing motifs with varying degrees of slipping along their long and short molecular axes while the diphenyl derivative packs into an edge-to-face herringbone arrangement. Powder diffraction data show that in thin films prepared by vacuum evaporation, molecules of the unsubstituted BADT are oriented nearly perpendicular to the substrate surface whereas the dialkylated derivatives adopt either multiple phases or new polymorphs. A thiahelicene prepared from the oxidative photocyclization of two isomers of 2,5-dithienyl-1,4-distyrylbenzene is described and the crystal structure reported.

Introduction

π-Conjugated organic compounds based on extended aromatic systems have attracted considerable attention over the past decade for their potential use as semiconductors in organic field-effect transistors (OFETs), organic light-emitting diodes (OLEDs), and photovoltaic cells.[1] Among the many classes that have been studied to date, oligoacenes are promising candidates for device applications since their linearly fused benzenoid structures give rise to a substantial increase in conjugation compared to their oligophenylene analogues.[2] Pentacene, for instance, is one of the most extensively studied oligoacenes as it exhibits superior charge carrier mobilities that make it suitable for application in OFETs.[3] Despite of their attractive electronic properties, oligoacenes are typically insoluble and chemically unstable making large scale solution-processing difficult, a clear drawback if these compounds are to be deposited using inkjet or pad printing processes. Recently, several researchers have developed strategies to improve the solubility of oligoacenes through chemical functionalization, while maintaining or improving both chemical stability and charge carrier mobility.[3] For example, thin films prepared from 6,13-bis(trialkylsilylethynyl)pentacenes are stable toward oxidation and exhibit hole mobilities up to 1.0 $cm^2\ V^{-1}\ s^{-1}$,[4] and 2,7-dialkyl[1]benzothieno[3,2-*b*][1]benzothiophenes have field effect mobilities of up to 2.7 $cm^2\ V^{-1}\ s^{-1}$.[5]

Incorporating thiophene into oligoacene frameworks is an alternative strategy in the development of new organic semi-

(1) Murphy, A. R.; Fréchet, J. M. J. *Chem. Rev.* **2007**, *107*, 1066–1096. (b) Kovac, J.; Peternai, L.; Lengyel, O. *Thin Solid Films* **2003**, *433*, 22–26.
(2) Bendikov, M.; Wudl, F.; Perepichka, D. F. *Chem. Rev.* **2004**, *104*, 4891–4946.
(3) Anthony, J. E. *Chem. Rev.* **2006**, *106*, 5028–5048.
(4) Payne, M. M.; Parkin, S. R.; Anthony, J. E.; Kuo, C.-C.; Jackson, T. N. *J. Am. Chem. Soc.* **2005**, *127*, 4986–4987.
(5) Ebata, H.; Izawa, T.; Miyazaki, E.; Takimiya, K.; Ikeda, M.; Kuwabara, H.; Yui, T. *J. Am. Chem. Soc.* **2007**, *129*, 15732–15733.

10.1021/jo900590u CCC: $40.75
Published on Web 05/26/2009

CHART 1

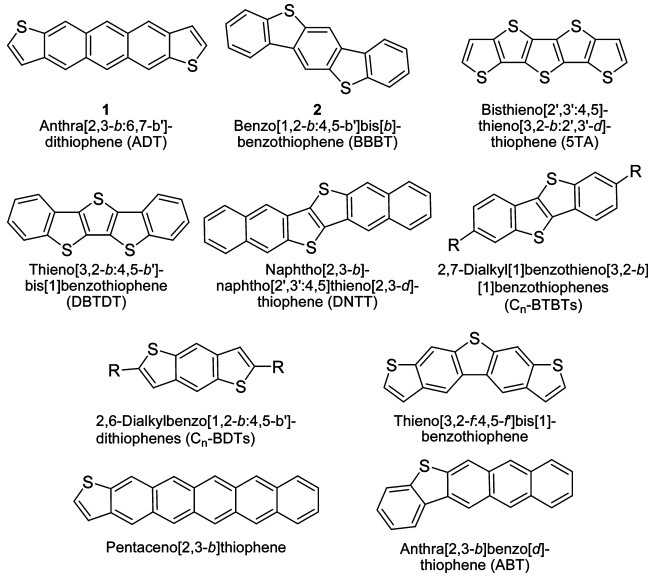

conductors since thiophene moieties can improve the extent of intermolecular $\pi-\pi$ overlap in the solid state, a feature that is intimately related to charge carrier mobility; see Chart 1 for some examples of known thiophene-based acenes.[5,6] Moreover, the site-selective reactivity of thiophene makes these molecules amenable to derivatization, leading to improved solubility, environmental stability, and processability. For instance, linear anthradithiophene (**1**),[6a−c] and benzo[1,2-*b*:4,5-*b*′]bis[1]benzothiophene (**2**),[6i] have hole mobilities that approach that of pentacene while showing improved oxidative stability and solubility. Recent efforts have shown that pentaceno[2,3-*b*]-thiophene is useful for application in OFETs.[6m] This is the most conjugated acene-based system to be used in a device application, overcoming the instability of hexacene that renders it impractical for application in thin-film transistors.

Recently, we communicated the synthesis of bent anthradithiophenes (BADTs) that are structurally analogous to dibenz[*a,h*]anthracene, a structural isomer of pentacene.[7] These compounds are soluble at room temperature, enabling their facile purification and processing. In this paper, the synthesis and spectroscopy of five BADTs and their thiophene-phenylene oligomer precursors are discussed in detail. The packing structures of the BADTs as single-crystals and thermally evaporated thin films are examined and compared, and the major product resulting from oxidative photocyclization of the novel *cis*,*cis*- and *trans*,*trans*-2,5-dithienyl-1,4-distyrylbenzenes is discussed.

SCHEME 1

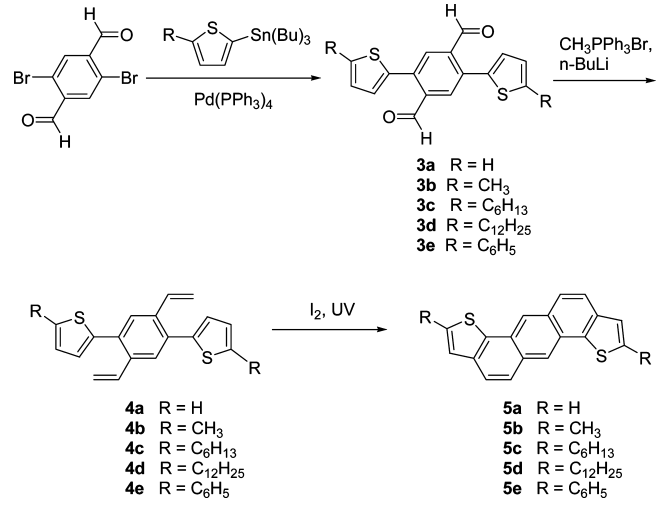

Results and Discussion

Synthesis, Characterization, and Spectroscopic Studies. The synthetic approach used to prepare BADTs **5a**−**e** is outlined in Scheme 1. Compounds **3a**−**e** were prepared via a 2-fold Stille cross-coupling reaction between 2,5-dibromoterephthalaldehyde and the appropriate 2-tributylstannylthiophene. The products were isolated as bright yellow solids after purification.

The ^{1}H NMR spectrum of **3b** is typical for the dialkylated derivatives. Singlets at δ 10.25 and 8.05 are assigned to the aldehyde C*H*O and aryl C*H* protons, respectively. Resonances at δ 6.94 and 6.86 are assigned to the thienyl C*H* protons and the singlet at δ 2.57 is assigned to the aliphatic CH_3 protons. The IR spectra of compounds **3a**−**e** exhibit strong stretching bands at 1680−1685 cm^{-1} confirming the integrity of the aldehydes after purification. The solution-phase UV−vis absorption spectra of **3a**−**e** in CH_2Cl_2 (see Supporting Information) contain three distinct absorption bands that are assigned to $\pi-\pi^*$ and n$-\pi^*$ electronic transitions. Introduction of alkyl-substituents to the thiophene moieties results in a small bathochromic shift of the absorption bands while the large shift observed for **3e** is attributed to an extension in conjugation that is imparted by the phenyl substituents. Compounds **3a**−**e** all exhibit green luminescence in solution with emission maxima between 490 and 548 nm, and quantum yields (Φ_F) of 0.39−0.92.

Wittig olefination of **3a**−**e** using methyltriphenylphosphonium bromide afforded compounds **4a**−**e** as white or yellow solids. The ^{1}H NMR spectra of **4a**−**e** show three distinct sets of doublet of doublets in the regions δ 7.00, 5.74, and 5.28 that are characteristic of the two-bond and three-bond coupling of the vinylic protons. All solution phase UV−vis absorption spectra in CH_2Cl_2 (see Supporting Information) show absorption maxima at 276−280 nm that are assigned to a $\pi-\pi^*$ transition involving the vinylic C═C chromophores. The lower energy shoulders are assigned to a $\pi-\pi^*$ transition involving the thiophene-phenylene oligomer.

BADTs **5a**−**e** were prepared by irradiating dilute benzene (or xylenes) solutions of **4a**−**e** with UV light (ca. 300 nm) in the presence of iodine. The reactions were monitored by UV−vis absorption spectroscopy and terminated when the

(6) (a) Lovinger, A. J.; Davis, D. D.; Ruel, R.; Torsi, L.; Dodabalapur, A.; Katz, H. E. *J. Mater. Res.* **1995**, *10*, 2958–2962. (b) Servet, B.; Horowitz, G.; Ries, S.; Lagorsse, O.; Alnot, P.; Yassar, A.; Deloffre, F.; Srivastava, P.; Hajlaoui, R. *Chem. Mater.* **1994**, *6*, 1809–1815. (c) Laquindanum, J. G.; Katz, H. E.; Lovinger, A. J. *J. Am. Chem. Soc.* **1998**, *120*, 664–672. (d) Cornil, J.; Beljonne, D.; Calbert, J.-P.; Brédas, J.-L. *Adv. Mater.* **2001**, *13*, 1053–1067. (e) Wex, B.; Kaafarani, B. R.; Schroeder, R.; Majewski, L. A.; Burckel, P.; Grell, M.; Neckers, D. C. *J. Mater. Chem.* **2006**, *16*, 1121–1124. (f) Yamamoto, T.; Takimiya, K. *J. Am. Chem. Soc.* **2007**, *129*, 2224–2225. (g) Gao, J.; Li, R.; Li, L.; Meng, Q.; Jiang, H.; Li, H.; Hu, W. *Adv. Mater.* **2007**, *19*, 3008–3011. (h) Kim, E.-G.; Coropceanu, V.; Gruhn, N. E.; Sánchez-Carrera, R. S.; Snoeberger, R.; Matzger, A. J.; Brédas, J.-L. *J. Am. Chem. Soc.* **2007**, *129*, 13072–13081. (i) Gao, P.; Beckmann, D.; Tsao, H. N.; Feng, X.; Enkelmann, V.; Pisula, W.; Müllen, K. *Chem. Commun.* **2008**, 1548–1550. (j) Izawa, T.; Miyazaki, E.; Takimiya, K. *Adv. Mater.* **2008**, *20*, 3388–3392. (k) Kashiki, T.; Miyazaki, E.; Takimiya, K. *Chem. Lett.* **2008**, *37*, 284–285. (l) Du, C.; Guo, Y.; Liu, Y.; Qiu, W.; Zhang, H.; Gao, X.; Liu, Y.; Qi, T.; Lu, K.; Yu, G. *Chem. Mater.* **2008**, *20*, 4188–4190. (m) Tang, M. L.; Mannsfeld, S. C. B.; Sun, Y.-S.; Becerril, H. A.; Bao, Z. *J. Am. Chem. Soc.* **2009**, *131*, 882–883.

(7) Pietrangelo, A.; MacLachlan, M. J.; Wolf, M. O.; Patrick, B. O. *Org. Lett.* **2007**, *9*, 3571–3573.

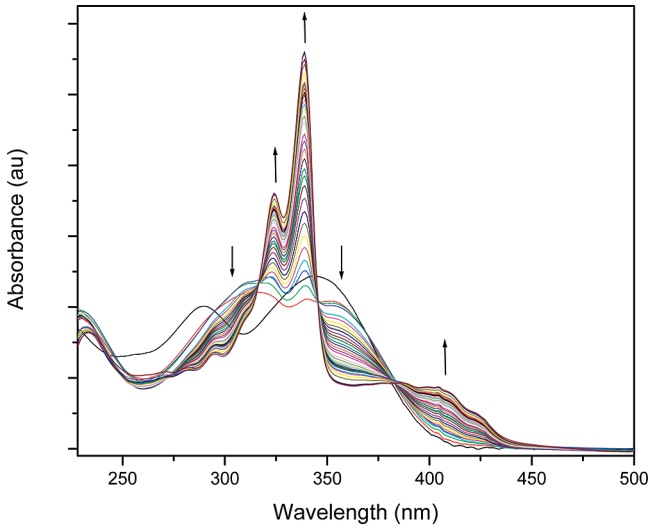

FIGURE 1. UV−vis absorption spectra of **5e** recorded at 30 s intervals during photolysis in benzene containing dissolved iodine at ca. 25 °C.

TABLE 1. UV-Vis Absorption and Emission Data for 5a−e

compound	solution absorption[a] λ_{max}/nm ($\varepsilon/10^2$ $M^{-1}cm^{-1}$)	solution emission[a] λ_{max}/nm	solid-state emission λ_{max}/nm	quantum yield[a] (Φ_f)
5a	304 (1429), 292 (600)	408	413	0.36
5b	309 (2179), 296 (963)	425	447	0.56
5c	311 (1295), 298 (529)	425	453	0.60
5d	311 (1620), 298 (670)	427	480	0.56
5e	324 (894), 339 (1560), 400 (180)	439	–	0.96

[a] CH_2Cl_2.

intensity of product absorption bands no longer increased with further irradiation. Figure 1 illustrates the conversion of **4e** to **5e** through a series of UV−vis absorption spectra taken at 30 s intervals during a typical photolysis experiment. Comparison with the absorption spectrum of pure **5e** (Supporting Information) confirms that this is the major product of the photolysis. Unlike the linear anthradithiophene (**1**, Chart 1) and its alkylated derivatives, compounds **5a−d** are synthesized as single isomers that are readily soluble in common organic solvents at room temperature enabling solution-based processing and purification. The diphenyl-derivative **5e**, however, was poorly soluble and therefore was best purified by sublimation. Compounds **5a−e** were all isolated as pale-yellow solids.

The solution phase UV−vis spectra of **5a−e** (Table 1) have nearly identical features and exhibit a vibronic structure that is similar to that of the all-phenyl analogue dibenz[*a*,*h*]anthracene.[8] These compounds exhibit blue fluorescence in solution (emission maxima = 408 − 439 nm; quantum yields (Φ_f) of 0.36−0.96) and green/blue fluorescence in the solid state.

The ^{1}H NMR spectrum of the dimethyl derivative **5b** has a resonance pattern that is consistent with BADTs functionalized at the α-position of the thiophene groups. A singlet at δ 8.59 is assigned to the thienyl β-hydrogens, which are shifted upfield from those of **5e** by 0.75 ppm. This is likely due to an extension of π-electron delocalization over the thienyl and the phenyl moieties in the latter. A singlet at δ 7.17 is assigned to the C*H* proton of the central phenyl ring of the anthracenyl moiety and the doublets at δ 7.86 and 7.72 are assigned to the remaining aromatic C*H* protons.

(8) Karcher, W.; Fordham, R. J.; Dubois, J. J.; Glaude, P. G. J. M.; Ligthart, J. A. M. *Spectral Atlas of Polycyclic Aromatic Compounds*; D. Reidel Publishing Company: Dordrecht, The Netherlands, 1985.

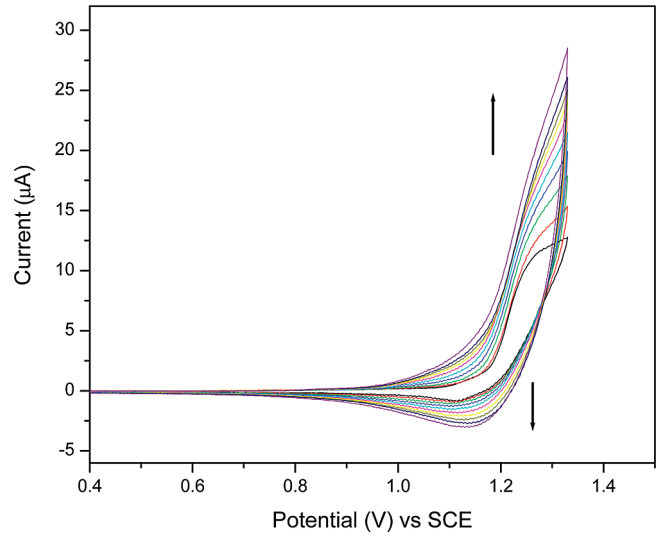

FIGURE 2. Cyclic voltammetry of **5a** in CH_2Cl_2 containing 0.1 M $[(n\text{-}Bu)_4N]ClO_4$. Scanned from +0.4 to + 1.3 V vs SCE for 10 cycles, scan rate = 100 mV s^{-1}.

Electrochemical Studies. The redox properties of BADTs **5a−d** were probed by cyclic voltammetry (CV). The parent BADT **5a** shows a single irreversible anodic wave at +1.2 V vs SCE that increases upon successive sweeps (Figure 2). The formation of a film on the working electrode suggests that radical cation species are generated during repeated cycling followed by polymerization affording poly-**5a**. Similar results have been observed for anthratetrathiophenes as well.[9]

To investigate the optical properties of the polymer, films of poly-**5a** were deposited on indium tin oxide (ITO) substrates. The UV−vis absorption spectrum of a poly-**5a** film on ITO exhibits a λ_{max} at 319 nm, only 15 nm red-shifted from the monomer (**5a**) suggesting that there is limited delocalization between monomeric units. In the cyclic voltammograms of dialkyl derivatives **5b−d**, all exhibit a single quasi-reversible redox wave that does not increase in intensity upon successive sweeps indicating that the alkyl substituents prevent polymerization and that the oxidative coupling of **5a** likely occurs through the α-positions of the thienyl groups.

Oxidative Photocyclization of 2,5-Dithienyl-1,4-distyrylbenzenes. To elucidate the scope of the synthetic approach, the oxidative photocyclization of 2,5-dithienyl-1,4-distyrylbenzenes **6** and **7** was investigated. The *cis*,*cis*-isomer **6** was prepared via a synthetic strategy also used to prepare the all-phenyl analogue *cis*,*cis*-2,5-diphenyl-1,4-distyrylbenzene.[10] This isomer was converted to the *trans*,*trans*-isomer **7** by heating **6** to reflux in *p*-xylene with catalytic iodine. These two isomers are unambiguously characterized as either *cis*,*cis* or *trans*,*trans* by both ^{1}H NMR and UV−vis absorption spectroscopy, and by comparison to the spectra of the all-*cis* and all-*trans* isomers of 2,5-diphenyl-1,4-distyrylbenzene.[10]

Irradiation of **7** in the presence of iodine was anticipated to afford a BADT with phenyl substituents extending from the

(9) Brusso, J. L.; Hirst, O. D.; Dadvand, A.; Ganesan, S.; Cicoira, F.; Robertson, C. M.; Oakley, R. T.; Rosei, F.; Perepichka, D. F. *Chem. Mater.* **2008**, *20*, 2484–2494.

(10) Xie, Z.; Yang, B.; Liu, L.; Li, M.; Lin, D.; Ma, Y.; Cheng, G.; Liu, S. *J. Phys. Org. Chem.* **2005**, *18*, 962–973.

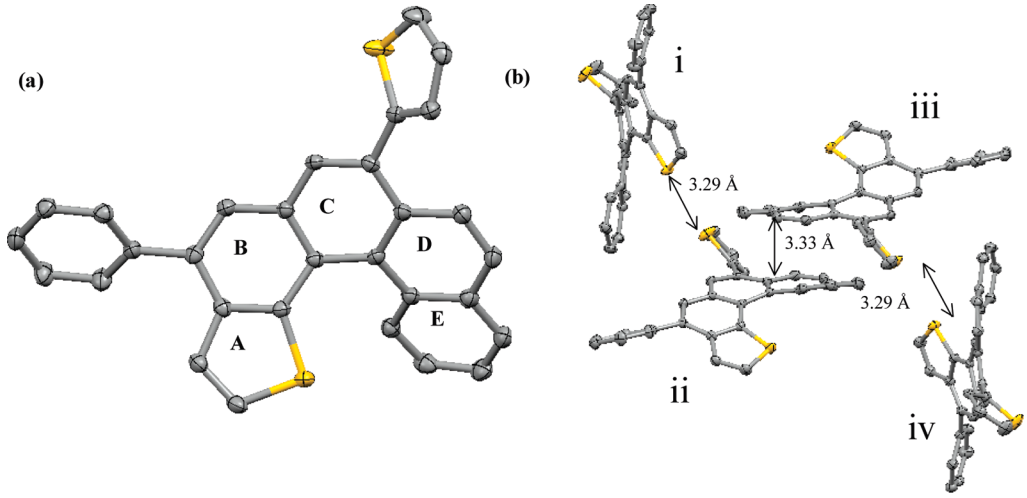

FIGURE 3. (a) Thermal ellipsoid plot of **8**. Thermal ellipsoids are drawn at 50% probability. The hydrogen atoms are omitted for clarity. (b) Packing diagram of **8**.

CHART 2

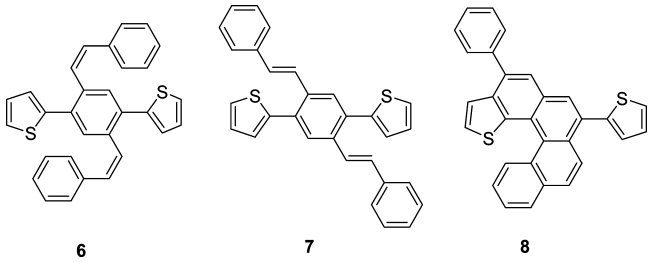

central anthracenyl group. To our surprise, irradiation of either **6** or **7** afforded a racemic mixture of the novel thiahelicene **8**. This product is formed through cyclization with the central aryl ring on one side, and with thiophene on the other. In contrast, the all-aryl analogue, 2,5-diphenyl-1,4-distyrylbenzene, undergoes cyclization exclusively at the central aryl ring to give 7,14-diphenyl-dibenz[*a,h*]anthracene.[11] Thiahelicenes are an emerging class of compounds that are interesting due to the site-selective reactivity of the thiophene group(s) that can be exploited to tune their electronic and chiroptical properties.[12]

Compound **8** was identified only after a single crystal X-ray diffraction (SCXRD) study. The thermal ellipsoid plot of **8** is shown in Figure 3. The thiahelicene **8** possesses C_1 symmetry and crystallizes as a racemate. Aromatic rings **B**−**E** all deviate from planarity while the thienyl ring **A** remains planar. A dihedral angle of 51° between the mean planes of **A** and **E** illustrates the large degree of twisting in the heterohelicene. For comparison, the dihedral angle between the terminal aromatic rings in trithia[5]heterohelicene[13] and [5]carbohelicene[14] are 37° and 49°, respectively. This large dihedral angle is somewhat surprising since a lower degree of steric crowding would be expected due to the orientation of the thiophene moiety **A** with its α and *β*-hydrogen atoms located on the periphery of the thiahelicene framework. The dihedral angles between the remaining mean planes of **8** are as follows: **A**−**B**: 11°, **B**−**C**: 15°, **C**−**D**: 12°, and **D**−**E**: 14°. The crystal packing of **8** is shown in Figure 3b. The S···S distance (ca. 3.29 Å) between alternating P and M enantiomers (i.e., *i*−*ii* and *iii*−*iv*) is shorter than the sum of their van der Waals radii (1.80 Å for S), suggesting the presence of intermolecular interactions that give rise to a one-dimensional chain-like structure. This stacking arrangement is unique since both thiophene moieties in **8** participate in intermolecular interactions, a feature that may be an attractive approach to self-assembly of thiahelicenes. In addition, a short intermolecular distance of 3.33 Å is observed between adjacent enantiomers, *ii* and *iii*, suggesting that *π*−*π* interactions also contribute to the intimate contact between P and M isomers in the single crystal.

Solid-State Crystal Structures and Packing. Elucidating the solid-state packing of BADTs in both single crystals and films grown by thermal evaporation is essential in understanding how the molecular assembly is influenced by substituents and, ultimately, to best optimize the solid-state arrangement for device applications.[6j] For the BADT derivatives that adopt a cofacial stacking arrangement, translational displacements between adjacent molecules were quantified using a method developed by Curtis and co-workers where slipping along the long and short molecular axis is described by pitch (**P**) and roll (**R**) angles (Figure 4).[15]

Crystals of **5a** and **5b** suitable for SCXRD studies were grown from cold CH_2Cl_2. Both compounds crystallize in the monoclinic $P2_1/n$ space group with two molecules in the unit cell. The rigid conjugated molecules are planar and show a small extent of cofacial overlap between adjacent molecules (Figure 5).

The pitch and roll angles of **5a** (see Table 2 for selected bond lengths) are 13° and 28°, respectively. An interplanar distance of 3.46 Å indicates the presence of *π*−*π* interactions along the intermolecular stacking axis. For comparison, dibenz[*a,h*]anthracene crystallizes into a herringbone arrangement ($P2_1$ or P_{cab}) with no intermolecular cofacial interactions.[16] Thus, the incorporation of thienyl groups appears to enhance *π*-stacking in the crystal lattice, a feature that is highly desirable in molecular organic semiconductors. In addition, the *π*-slipped stacks are aligned into edge-to-face herringbone arrays where four intermolecular close-contacts are observed between each molecule of **5a** and four others in adjacent stacks (Figure 5c). For instance, the distance between the sulfur atoms in a molecule of **5a** (i.e.,

(11) Xie, Z.; Yang, B.; Cheng, G.; Liu, L.; He, F.; Shen, F.; Shen, F.; Ma, Y.; Liu, S. *Chem. Mater.* **2005**, *17*, 1287–1289.
(12) Collins, S. K.; Vachon, M. P. *Org. Biomol. Chem.* **2006**, *4*, 2518–2524.
(13) Nakagawa, H.; Yamada, K.; Kawazura, H.; Miyamae, H. *Acta Cryst, Sect. C: Cryst. Struct. Commun.* **1984**, *C40*, 1039–1041.
(14) Goedicke, C.; Stegemeyer, H. *Tetrahedron Lett.* **1970**, *11*, 937–940.
(15) Curtis, M. D.; Cao, J.; Kampf, J. W. *J. Am. Chem. Soc.* **2004**, *126*, 4318–4328.

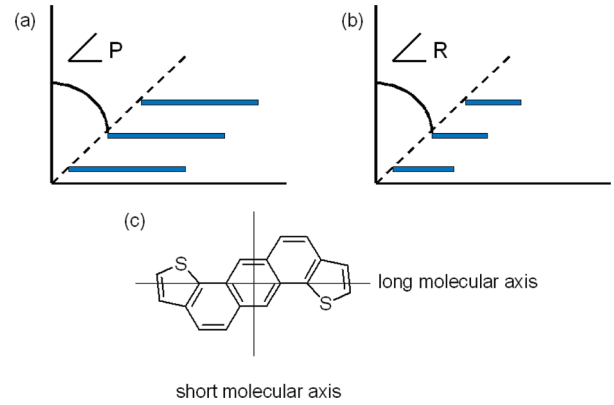

FIGURE 4. (a) Pitch angle (**P**) describing intermolecular slipping along the long molecular axis (view down short molecular axis). (b) Roll angle (**R**) describing intermolecular slipping along the short molecular axis (view down long molecular axis). (c) Long and short molecular axes of **5a**.

S1 and S1*) and a single C9 atom from two adjacent molecules is 3.47 Å, a distance shorter than the sum of their van der Waals radii (3.55 Å). This same distance is observed between the C9 and C9* atoms of each molecule and the sulfur atoms of two additional molecules. Interestingly, this contact distance is shorter than those observed between close-carbon contacts in adjacent molecules of pentacene (3.6−3.8 Å),[17] and suggests that a single crystal of **5a** may have a two-dimensional electronic structure.

An interplanar distance of 3.28 Å between adjacent molecules of **5b** (Figure 5d) indicates the presence of $\pi-\pi$ interactions along the intermolecular stacking axis. The pitch and roll angles are 45 and 44°, respectively; hence, it appears that the methyl substituents induce a large degree of slipping along both the short and long molecular axes compared to the parent. In addition, there is no evidence of close contacts between adjacent stacks. This packing feature has been observed in **2**[18] and suggests that a single crystal of **5b** may have a one-dimensional electronic structure.

Single crystals of the dihexyl (**5c**) and didodecyl (**5d**) derivatives were grown from cold chloroform and their structures determined by SCXRD. Compound **5c** crystallizes into the monoclinic $P2_1/c$ space group with two molecules in the unit cell. In the crystal lattice, both hexyl chains are in a conformation that extends above and below the aromatic plane of the BADT framework at 39° angles (Figure 6).

Unlike **5a** and **5b**, there is no evidence of cofacial $\pi-\pi$ interactions in the crystalline phase of **5c** due to the large degree of slipping (pitch angle, 15°; roll angle, 72°) between adjacent coplanar molecules along their short molecular axis (Figure 6). This could be due to steric effects imparted by the hexyl substituents, a phenomenon that has also been observed in a dihexyloxy-derivatized fluorinated tetracene.[19]

The didodecyl derivatized BADT **5d** crystallizes into the triclinic P-1 space group with a single molecule in the unit cell (graphic is shown in ref 7). Functionalizing the thienyl α-positions with dodecyl chains regenerates the cofacial stacking arrangement with pitch and roll angles of 19° and 48°, respectively. In the crystal lattice, both dodecyl chains are in a conformation that extends above and below the aromatic plane of the BADT framework at 46° angles. The interplanar stacking distance of 3.49 Å is indicative of $\pi-\pi$ interactions along the stacking axis. In the solid state, the molecules are organized into a lamellar packing arrangement with the stacks separated by insulating dodecyl chains. The lack of contact between the π-stacks suggests a one-dimensional electronic structure in the crystal.

Single crystals of the diphenyl-derivatized BADT **5e** were grown from a solution of **5e** in *p*-xylene that was heated to reflux and subsequently cooled to room temperature; the structure determined by SCXRD is shown in Figure 7. The rigid conjugated structure is slightly twisted with the pendant phenyl rings rotated out of the plane of the thiophene groups at an angle of 21°. In the solid state, **5e** adopts an edge-to-face herringbone packing motif where the tilt angle between two mean planes of the BADT framework is 33°, compared to 45° in the all-carbon analog dibenz[*a,h*]anthracene[16] and 52° in pentacene.[17] There are eight intermolecular close-contacts in these edge-to-face structures that link a molecule of **5e** with four others in the lattice. The two types of contacts are shown in Figure 7b. The closest intermolecular C−C distances are 3.29 and 3.33 Å. These distances are shorter than the closest intermolecular C−C distances observed in pentacene,[17] phenyl-substituted pentacenes,[20] and dibenz[*a,h*]anthracene,[16] and may lead to strong electronic coupling between adjacent molecules in the crystalline lattice.

Powder X-Ray Diffraction (PXRD) Analyses of BADT Films. The PXRD pattern of a film of **5a** prepared by vacuum evaporation exhibits two strong reflections corresponding to the (10−1) and (20−2) planes assigned from the diffraction pattern calculated from the SCXRD data. The thin film is highly crystalline, with reflections indicating that the molecules are oriented with their long molecular axes nearly perpendicular (ca. 77°) to the substrate surface, a phenomenon seen in oligothiophenes as well as in the linear anthradithiophenes prepared by Katz and co-workers.[6a,c] This packing orientation is favorable for electronic device applications as the direction of the π-orbital overlap is parallel to the substrate surface and coincides with the plane in which a current must flow.

The XRD pattern of a film of **5d** prepared by vacuum evaporation exhibits six strong reflections that correspond to the (001) through (006) planes (Figure 8b). The molecules are oriented with their long molecular axes inclined approximately 47° with respect to the (001) plane that is parallel to the substrate surface. These reflections are consistent with those observed in films prepared from the didodecyl derivative of **1**, suggesting that this compound packs into a similar arrangement.[6c]

The XRD pattern of a film of **5b** suggests that there are two phases present (Figure 8c). The two sharp reflections at $2\theta =$ 11.4 and 23.0° correspond to the (10−1) and (20−2) planes of the $P2_1/n$ space group. These assignments are supported by the SCXRD data and are consistent with the diffraction pattern

(16) (a) Iball, J. *Nature* **1936**, *137*, 361. (b) Iball, J.; Morgan, C. H.; Zacharias, D. E. *J. Chem. Soc., Perkin Trans. 2: Phys. Org. Chem.* **1975**, 1271–1272. (c) Krishnan, K. S.; Banerjee, S. *Z. Kristallogr.* **1935**, *91*, 170–172. (d) Robertson, J. M.; White, J. G. *J. Chem. Soc.* **1947**, 1001–1010. (e) Robertson, J. M.; White, J. G. *J. Chem. Soc.* **1956**, 925–931.

(17) (a) Campbell, R. B.; Robertson, J. M.; Trotter, J. *Acta Crystallogr.* **1962**, *15*, 289–90. (b) Holmes, D.; Kumaraswamy, S.; Matzger, A. J.; Vollhardt, K. P. C. *Chem.—Eur. J.* **1999**, *5*, 3399–3412. (c) Siegrist, T.; Kloc, C.; Schön, J. H.; Batlogg, B.; Haddon, R. C.; Berg, S.; Thomas, G. A. *Angew. Chem., Int. Ed.* **2001**, *40*, 1732–1736. (d) Mattheus, C. C.; Dros, A. B.; Baas, J.; Meetsma, A.; de Boer, J. L.; Palstra, T. T. M. *Acta Cryst., Sect. C: Cryst. Struct. Commun.* **2001**, *C57*, 939–941.

(18) Ebata, H.; Miyazaki, E.; Yamamoto, T.; Takimiya, K. *Org. Lett.* **2007**, *9*, 4499–4502.

(19) Chen, Z.; Müller, P.; Swager, T. M. *Org. Lett.* **2006**, *8*, 273–276.

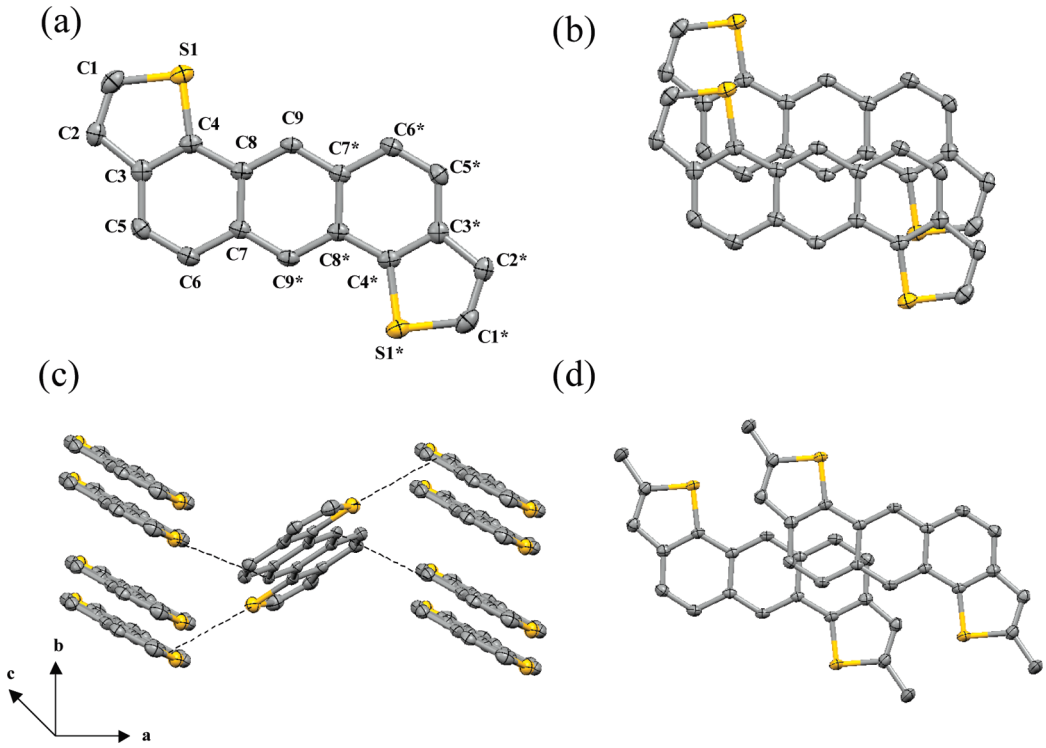

FIGURE 5. (a) Thermal ellipsoid plot of **5a**. The hydrogen atoms are omitted for clarity. Thermal ellipsoids are drawn at 50% probability. (b) View down the stacking axis of two cofacial molecules of **5a**. (c) Crystal packing of **5a**. Dashed lines illustrate short contacts (ca. 3.47 Å). (d) View down the stacking axis of two cofacial molecules of **5b**.

TABLE 2. Selected Bond Lengths of BADT 5a

bond length /Å		bond length / Å	
C(1)−C(2)	1.347(3)	C(4)−S1	1.725(2)
C(1)−S(1)	1.715(2)	C(5)−C(6)	1.351(3)
C(2)−C(3)	1.452(3)	C(6)−C(7)	1.436(3)
C(3)−C(4)	1.388(3)	C(7)−C(9)	1.394(3)
C(3)−C(5)	1.429(3)	C(7)−C(8)	1.435(3)
C(4)−C(8)	1.432(3)	C(8)−C(9)	1.389(3)

obtained from crystals of **5b**. The molecules are inclined approximately 35° with respect to the (10−1) plane that is parallel to the substrate surface. The additional reflections observed at $2\theta = 10.8$ and 22.4° are absent in both the calculated and experimental diffraction patterns and are shifted approximately 0.6° from the reflections assigned to the (10−1) and (20−2) planes. Similar features have been observed in the XRD analysis of a pentacene thin-film grown onto a silica substrate using molecular beam deposition techniques.[21] These features have been attributed to the coexistence of two phases, a "thin-film" phase and a "single-crystal" phase that form under certain deposition conditions.

The diffraction pattern obtained from a film of **5c** exhibits four sharp reflections at $2\theta = 5$, 10, 15, and 20° (Figure 8d). These reflections are inconsistent with those calculated from the SCXRD data and those obtained experimentally from crystals of **5c** suggesting that the dihexyl-derivatized BADT adopts a different packing motif in the evaporated film. Interestingly, this diffraction pattern is very similar to that obtained from a film of **5d** (Figure 8b). The similarities between the diffraction patterns suggests that, like the didodecyl derivative, the dihexyl derivative also adopts a lamellar packing arrangement in the film.

Solid-State Absorption and Luminescence Properties of Films. The solid-state UV−vis absorption spectra of drop-cast films of **5a**−**d** exhibit nearly identical features with λ_{max} ranging between 280 and 311 nm. Representative spectra of **5a** and **5d** are shown in Figure 9. The high energy peaks in the solid-state emission spectrum of **5a** and **5d** are similar to those found in the solution phase spectrum. At longer wavelengths, however, the emission intensity from the thin film is greater and a new peak is present at 486 nm. The solid-state emission spectrum of **5d** is red-shifted relative to solution, a feature that is attributed to intermolecular interactions in the microcrystalline film,[22] where π-stacking has been observed in the solid-state structures.

Conclusions

A new series of bent anthradithiophenes (BADTs) **5a**−**e** has been prepared via photochemical cyclization of **4a**−**e** using iodine as the oxidant. Apart from the diphenyl derivative **5e**, all the new BADTs are soluble in common organic solvents including hexanes, CH_2Cl_2, and chloroform. Cyclic voltammetry revealed that **5a** polymerizes electrochemically upon successive potential sweeps to afford thin films while the dialkyl derivatized BADTs **5b**−**d** exhibit a similar quasi-reversible redox wave but do not electropolymerize, supporting the conclusion that **5a** polymerizes through the α-carbon of the thienyl groups. In order to extend the scope of the synthetic strategy used here, oxidative photocyclization reactions were carried out on the *cis*,*cis*- and *trans*,*trans*-2,5-dithienyl-1,4-distyrylbenzenes **6** and **7**. Both reactions yielded a racemic mixture of the thiahelicene **8** which

(20) Miao, Q.; Chi, X.; Xiao, S.; Zeis, R.; Lefenfeld, M.; Siegrist, T.; Steigerwald, M. L.; Nuckolls, C. *J. Am. Chem. Soc.* **2006**, *128*, 1340–1345.
(21) Dimitrakopoulos, C. D.; Brown, A. R.; Pomp, A. *J. Appl. Phys.* **1996**, *80*, 2501–2508.
(22) Dabestani, R.; Ivanov, I. N. *Photochem. Photobiol.* **1999**, *70*, 10–34.
(23) Xia, C.; Advincula, R. C. *Macromolecules* **2001**, *34*, 6922–6928.

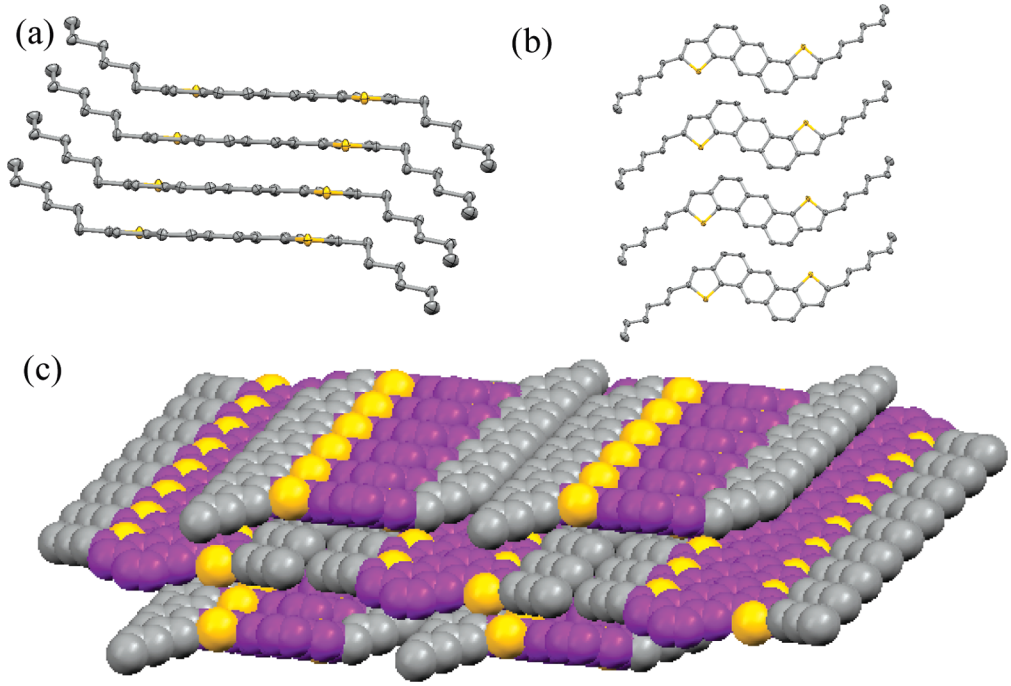

FIGURE 6. Packing diagram of **5c**. (a) View along short molecular axis. The hydrogen atoms are omitted for clarity. Thermal ellipsoids are drawn at 50% probability. (b) View perpendicular to the molecular plane of the stacking axis. (c) Space-filling diagram of **5c**. Sulfur atoms are yellow, sp^3-hybridized carbon atoms are gray, and sp^2-hybridized carbon atoms are purple.

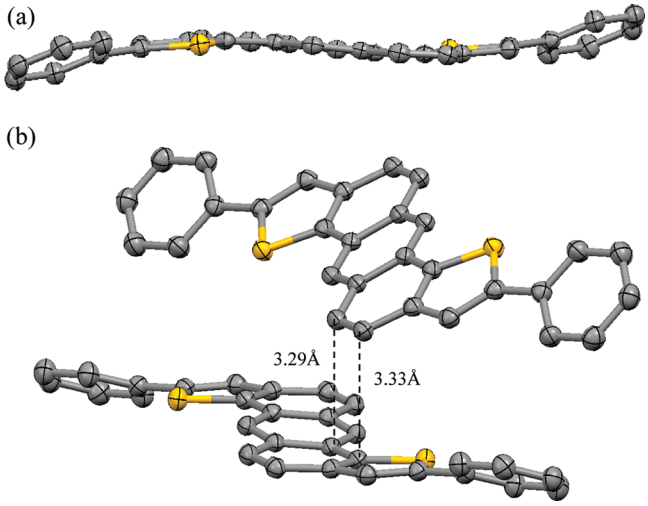

FIGURE 7. (a) View down the short molecular axis of **5e**. The hydrogen atoms are omitted for clarity. Thermal ellipsoids are drawn at 50% probability. (b) Crystal structure of **5e** showing two of the eight close contacts between the edge of one acene and the face of another.

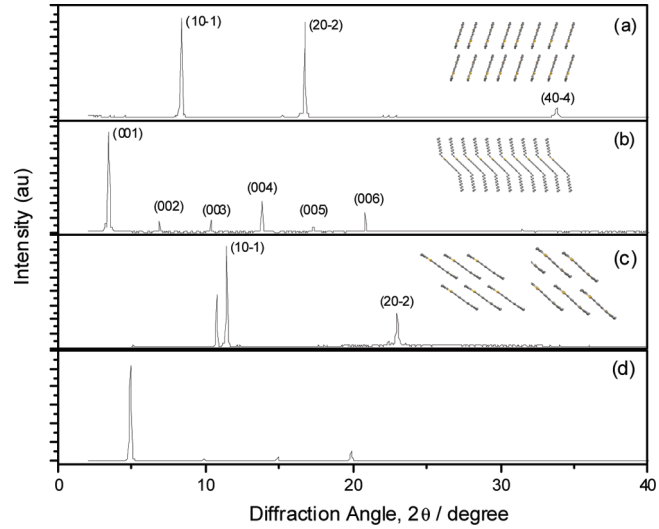

FIGURE 8. X-ray diffractograms and schematic representations of the structural orientation of (a) **5a**, (b) **5d**, (c) **5b**, and (d) **5c** on glass substrates (parallel to the x-axes) deposited by vacuum evaporation.

has been characterized by a variety of spectroscopic techniques and SCXRD studies.

The solid-state packing motif of crystalline BADT **5a** shows a slipped cofacial stacking arrangement with $\pi-\pi$ interactions along the intermolecular stacking axis. This motif was not observed in the all-carbon analog, dibenz[*a*,*h*]anthracene, suggesting that the thiophene units enhance π-stacking in the crystal lattice. The dialkyl derivatized BADTs **5b**−**d** adopt similar packing motifs with varying degrees of slipping along their long and short molecular axes. The diphenyl derivative, **5e**, packs into an edge-to-face herringbone arrangement that is common in many phenyl-substituted and unsubstituted oligoacenes.

Single-crystal and powder XRD studies demonstrated that films prepared via vacuum evaporation are highly crystalline with a preferred specific orientation relative to the substrate surface. Films of **5a** and **5d** possess reflections that are consistent with the single crystal data suggesting that packing in the film is similar to packing in the single crystal. In addition, molecules of **5a** are oriented nearly perpendicular to the substrate surface, a feature that is highly desirable for application in thin-film OFETs. Films of the dimethyl derivative showed some reflections that were consistent with the single-crystal data and others that could not be attributed to this structure, suggesting the presence of two phases in the film. Films of the dihexyl derivative **5c** showed a set of reflections that were inconsistent

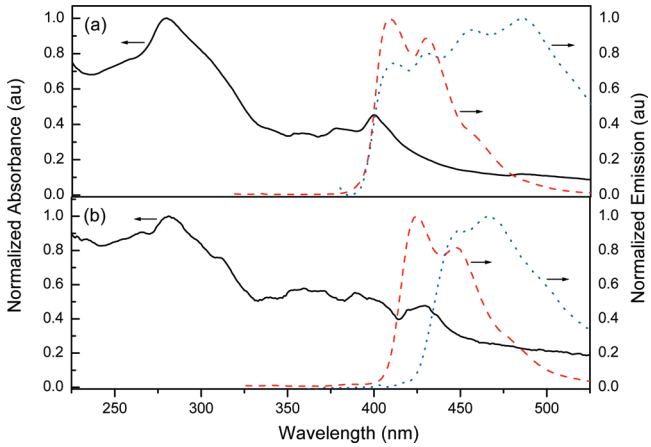

FIGURE 9. (a) Solid-state UV−vis absorption spectrum of **5a** (—). Emission spectrum of **5a** in solution (---, λ_{ex} = 304 nm) and as a thin film (•••, λ_{ex} = 300 nm). (b) Solid-state UV−vis absorption spectrum of **5d** (—). Emission spectrum of **5d** in solution (---, λ_{ex} = 311 nm) and as a thin film (•••, λ_{ex} = 281 nm). All spectra were obtained at ca. 25 °C.

with those calculated from the single-crystal data suggesting the presence of a new polymorph in the thin film.

Experimental Section

General. Chromium trioxide, 2-tributylstannylthiophene, methyltriphenylphosphonium bromide, anhydrous DMF, $Pd(PPh_3)_4$, and benzyltriphenylphosphonium chloride were purchased from standard suppliers. THF was distilled from sodium and benzophenone under N_2. 2,5-Dibromoterephthalaldehyde,[23] 5-methyl-2-tributylstannylthiophene,[24] 5-hexyl-2-tributylstannylthiophene,[25] 5-dodecyl-2-tributylstannylthiophene,[26] and 5-phenyl-2-tributylstannylthiophene[27] were prepared according to literature procedures. The syntheses of **3a**−**d**, **4a**−**d** and **5a**−**d** were reported in a previous communication.[7] All reactions were carried out under a dinitrogen atmosphere unless otherwise noted.

Synthesis. 2,5-Bis(5-phenyl-2-thienyl)terephthalaldehyde (3e). A round-bottom Schlenk flask was charged with 2,5-dibromoterephthalaldehyde (0.300 g, 1.03 mmol), $Pd(PPh_3)_4$ (0.12 g, 0.010 mmol), 2-tributylstannyl-5-phenylthiophene (1.4 g, 3.1 mmol) and anhydrous DMF (30 mL) and heated to 80 °C with stirring for 36 h. The reaction mixture was then cooled to room temperature, diluted with Et_2O, and filtered through Celite. The organic phase was washed with brine and water, then dried over Na_2SO_4. After filtration, the solvent was removed to yield the crude product, which was chromatographed on silica using a hexanes/CH_2Cl_2 (1:1) solvent mixture as the eluent (R_f = 0.70). The orange product was isolated in 43% yield (0.20 g, 0.44 mmol). ^{1}H NMR (CD_2Cl_2, 400 MHz) δ 10.36 (2H, s), 8.19 (2H, s), 7.70 (4H, m), 7.44 (6H, m), 7.36 (2H, t, $^3J_{HH}$ = 7.39 Hz), 7.16 (2H, d, $^3J_{HH}$ = 3.72 Hz). ^{13}C NMR (CD_2Cl_2, 100 MHz) δ 191.5, 148.0, 137.42, 137.26, 134.2, 131.29, 131.26, 129.7, 128.8, 126.4, 124.7. EI-MS: m/z = 450 (M^+, 100%). UV−vis (CH_2Cl_2): λ_{max} (ϵ) = 270 (22400), 333 (29300), 413 (11400) nm (L mol^{-1} cm^{-1}). IR (neat): ν = 1681, 1476, 1444, 1379, 1325, 1270, 1251, 1146, 1079, 903, 822, 812, 759, 689, 644, 634, 586, 553, 532 cm^{-1}. Mp > 230 °C. Anal. Calcd for $C_{28}H_{18}O_2S_2$: C, 74.64; H, 4.03. Found: C, 74.24; H, 4.04.

2,5-Bis(5-phenyl-2-thienyl)-1,4-divinylbenzene (4e). A suspension of methyltriphenylphosphonium bromide (0.30 g, 0.84 mmol) and 60 mL of anhydrous THF in a 250 mL round-bottom Schlenk flask was cooled to 0 °C, then 0.62 mL of *n*-BuLi (1.6 M in hexanes; 0.99 mmol) was added dropwise. After 30 min of stirring, a solution of **3e** (0.15 g, 0.33 mmol) dissolved in 30 mL of anhydrous THF was added. The combined solution was then warmed to room temperature and left to stir for 24 h. Solvent was then removed under reduced pressure and the product purified by column chromatography using CH_2Cl_2 as the eluent (R_f = 1.00). The product was isolated as a white solid in 84% yield (0.125 g, 0.280 mmol).^{1}H NMR (CD_2Cl_2, 400 MHz) δ 7.74 (2H, s), 7.67 (4H, d, $^3J_{HH}$ = 7.40 Hz), 7.42 (4H, t, $^3J_{HH}$ = 7.44 Hz), 7.36 (2H, d, $^3J_{HH}$ = 3.67 Hz), 7.32 (2H, t, $^3J_{HH}$ = 7.37 Hz), 7.13 (2H, d, $^3J_{HH}$ = 3.67 Hz), 7.08 (2H, dd, $^3J_{HH}$ = 17.47 Hz, $^3J_{HH}$ = 11.03 Hz), 5.82 (2H, d, $^3J_{HH}$ = 17.42 Hz), 5.35 (2H, d, $^3J_{HH}$ = 11.53 Hz). ^{13}C NMR (CD_2Cl_2, 100 MHz) δ 145.4, 141.5, 136.4, 135.8, 134.7, 133.2, 129.54, 129.49, 128.88, 128.23, 126.2, 124.0, 116.6. EI-MS: m/z = 446.1 (M^+, 100%). UV−vis (CH_2Cl_2): λ_{max} (ϵ) = 344 nm (25300), 291 nm (20400) (L mol^{-1} cm^{-1}). IR (neat): ν = 1592, 1485, 1460, 1444, 1408, 1379, 1337, 1254, 1159, 1099, 1075, 982, 940, 920, 897, 889, 842, 812, 753, 686, 615 cm^{-1}. Mp 209 °C. Anal. Calcd for $C_{30}H_{22}S_2$: C, 80.68; H, 4.96. Found: C, 80.41; H, 5.07.

Anthra(1,2-b:5,6-b′)di-5-phenylthiophene (5e). A 500 mL quartz flask was charged with **4e** (0.080 g, 0.18 mmol), iodine (0.25 g, 1.0 mmol), and 200 mL of xylenes sparged with dinitrogen gas. The flask was irradiated in a photoreactor (300 nm lamps) for 72 h, and UV−vis spectroscopy confirmed that the reaction was complete. For workup, the organic solution was washed with aqueous sodium dithionite solution and the solvent removed under vacuum. Benzene (60 mL) was added to the brown solid that remained, and the product was isolated by filtration and washed with hexanes. The product was sublimed under vacuum for further purification, yielding a yellow solid (32 mg, 40%). ^{1}H NMR (DMSO-d_6, 400 MHz) δ 8.89 (2H, s), 8.13 (2H, d, $^3J_{HH}$ = 8.74 Hz), 8.08 (2H, s), 7.95 (2H, d, $^3J_{HH}$ = 8.73 Hz), 7.89 (4H, d, $^3J_{HH}$ = 7.46 Hz), 7.54 (4H, t, $^3J_{HH}$ = 7.50 Hz), 7.43 (2H, t, $^3J_{HH}$ = 7.24 Hz). EI-MS: m/z = 442 (M^+, 100%). HRMS (EI): Calcd for $C_{30}H_{18}S_2$: 442.08499; Found: 442.08404. UV−vis (CH_2Cl_2): λ_{max} (ϵ) = 324 (89400), 339 (156200), 400 (17500) nm (L mol^{-1} cm^{-1}). IR (neat): ν = 1071, 1025, 879, 835, 801, 757, 745, 689, 608 cm^{-1}. Mp > 230 °C.

Cis,cis-2, 5-bis(2-thienyl)-1,4-distyrylbenzene (6). A suspension of benzyltriphenylphosphonium chloride (0.313 g, 0.805 mmol) and 30 mL of anhydrous THF in a 250 mL round-bottom Schlenk flask was cooled to 0 °C and left to stir for 30 min. With stirring, 0.46 mL of *n*-BuLi (1.6 M in hexanes) was added dropwise. After an additional 30 min of stirring, a solution of 2,5-di(2-thienyl)-terephthalaldehyde **3a** (0.100 g, 0.335 mmol) dissolved in 30 mL of anhydrous THF was added. The combined solution was warmed to room temperature and left to stir for 24 h. Solvent was then removed under reduced pressure and the product purified by column chromatography using CH_2Cl_2 as the eluent (R_f = 0.97). The *cis,cis*-isomer was isolated as a white solid (0.12 g, yield 80%). ^{1}H NMR (CD_2Cl_2, 400 MHz) δ 7.43 (2H, s), 7.30 (12H, m), 7.05 (2H, d, $^3J_{HH}$ = 3.55 Hz), 7.00 (2H, dd, $^3J_{HH}$ = 5.02 Hz, $^3J_{HH}$ = 3.67 Hz), 6.71 (2H, d, $^3J_{HH}$ = 12.09 Hz), 6.67 (2H, d, $^3J_{HH}$ = 12.09 Hz). ^{13}C NMR (CD_2Cl_2, 100 MHz) δ 142.4, 137.5, 135.2, 133.0, 132.2, 132.1, 130.2, 129.5, 128.8, 127.86, 127.83, 127.6, 126.5. EI-MS: m/z = 446 (M^+, 100%). UV−vis (CH_2Cl_2): λ_{max} (ϵ) = 311 nm (27400) (L mol^{-1} cm^{-1}). IR (KBr): ν = 1481, 1438, 1400, 1382, 1241, 1241, 1213, 1072, 1056, 919, 904, 846, 831, 773, 744, 735, 690, 538, 505, 471, 445 cm^{-1}. Mp 175−177 °C. Anal. Calcd for $C_{30}H_{22}S_2$: C, 80.68; H, 4.96. Found: C, 80.79, H, 5.17.

Trans,trans-2, 5-bis(2-thienyl)-1,4-distyrylbenzene (7). Compound **6** (0.12 g, 0.27 mmol) was dissolved in 10 mL of xylenes with a catalytic amount of I_2 and heated to reflux for 12 h. After

(24) Berridge, R.; Wright, S. P.; Skabara, P. J.; Dyer, A.; Steckler, T.; Argun, A. A.; Reynolds, J. R.; Harrington, R. W.; Clegg, W. *J. Mater. Chem.* **2007**, *17*, 225–231.

(25) Jousselme, B.; Blanchard, P.; Gallego-Planas, N.; Levillain, E.; Delaunay, J.; Allain, M.; Richomme, P.; Roncali, J. *Chem.—Eur. J.* **2003**, *9*, 5297–5306.

(26) Wilson, P.; Lacey, D.; Sharma, S.; Worthington, B. *Mol. Cryst. Liq. Cryst. Sci. Tech.* **2001**, *368*, 279–292.

(27) Li, J. J.; Carson, K. G.; Trivedi, B. K.; Yue, W. S.; Ye, Q.; Glynn, R. A.; Miller, S. R.; Connor, D. T.; Roth, B. D.; Luly, J. R.; Low, J. E.; Heilig, D. J.; Yang, W.; Qin, S.; Hunt, S. *Bioorg. Med. Chem.* **2003**, *11*, 3777–3790.

cooling, the product was precipitated upon addition to methanol and isolated on a Büchner funnel (0.10 g, 83%). ^{1}H NMR (CD_2Cl_2, 400 MHz) δ 7.85 (2H, s), 7.47 (6H, m), 7.40 (2H, d, $^3J_{HH}$ = 16.24 Hz), 7.35 (4H, m, aromatic C*H*), 7.22 (2H, dd, $^3J_{HH}$ = 3.51 Hz, $^3J_{HH}$ = 1.17 Hz), 7.18 (2H, dd, $^3J_{HH}$ = 5.06 Hz, $^3J_{HH}$ = 3.57 Hz), 7.14 (2H, d, $^3J_{HH}$ = 16.23 Hz). ^{13}C NMR (CD_2Cl_2, 100 MHz) δ 142.3, 138.0, 135.8, 133.8, 131.1, 129.3, 129.0, 128.44, 128.33, 128.07, 127.29, 127.21, 126.8. EI-MS: m/z = 446 (M^+, 100%). UV−vis (CH_2Cl_2): λ_{max} (ϵ) = 312 (43600), 348 (43700) nm (L mol^{-1} cm^{-1}). IR (KBr): ν = 1594, 1493, 1446, 1390, 1315, 1235, 1207, 983, 946, 897, 854, 840, 755, 710, 731, 689, 669, 590, 513, 484 cm^{-1}. Mp > 220 °C. Anal. Calcd for $C_{30}H_{22}S_2$: C, 80.68; H, 4.96. Found: C, 80.31; H, 5.30.

Thiahelicene (8). A 500 mL quartz flask was charged with **7** (0.080 g, 0.18 mmol), iodine (0.090 g, 0.36 mmol), and 250 mL of benzene sparged with dinitrogen gas. The flask was irradiated in a photoreactor (300 nm lamps) for 2 weeks. After purification by flash column chromatography (1:1 hexanes:CH_2Cl_2), side products of lower solubility that eluted with the helicene were separated by precipitation from cold hexanes/ CH_2Cl_2 (1:1) solutions. The final product is a gray solid (yield 20%) that decomposes in solution at room temperature. R_f = 0.80 (hexanes/ CH_2Cl_2 (1:1)). ^{1}H NMR (CD_2Cl_2, 400 MHz) δ 8.85 (1H, d, $^3J_{HH}$ = 8.44 Hz), 8.20 (1H, d, $^3J_{HH}$ = 8.84 Hz), 8.10 (1H, s), 8.05 (1H, d, $^3J_{HH}$ = 7.85) 7.95 (2H, m), 7.78 (2H, d, $^3J_{HH}$ = 6.94 Hz), 7.68 (1H, t, $^3J_{HH}$ = 6.91 Hz), 7.58 (2H, t, $^3J_{HH}$ = 7.24 Hz), 7.50 (4H, m), 7.35 (1H, d, $^3J_{HH}$ = 5.57 Hz), 7.32 (1H, dd, $^3J_{HH}$ = 3.49 Hz, $^3J_{HH}$ = 1.17 Hz), 7.25 (1H, dd, $^3J_{HH}$ = 5.15 Hz, $^3J_{HH}$ = 3.50 Hz). ^{13}C NMR (CD_2Cl_2, 100 MHz) δ 141.8, 141.0, 139.3, 139.1, 137.9, 133.2, 131.42, 131.37, 130.76, 130.72, 130.3, 129.9, 129.2, 128.82, 128.67, 128.33, 128.23, 128.05, 128.01, 127.9, 127.7, 126.6, 125.43, 125.36, 125.03, 124.83, 124.15, 123.89. EI-MS: m/z = 442 (M^+, 100%). HRMS (EI): Calcd for $C_{30}H_{18}S_2$: 442.08499; Found: 442.08444. UV−vis (CH_2Cl_2): λ_{max} (ϵ) = 319 (33917), 269 (20785), 243 (30345) nm (L mol^{-1} cm^{-1}). IR (neat): ν = 1495, 1434, 1386, 1243, 1219, 1081, 1026, 905, 853, 838, 820, 798, 770, 760, 748, 722, 711, 694, 666, 643, 612, 591, 554, 521, 504 cm^{-1}. Mp 195 °C.

X-Ray Crystallographic Analysis. Crystallographic data for **3b**, **5b**−**e**, and **8** are included in the Supporting Information. Data for **5a** are available in ref 7.

Single crystals of **3b**, **5b**−**d**, and **8** were grown from cold CH_2Cl_2 or chloroform. Crystals were mounted on glass fibers and the data collected at 173(1) K on a diffractometer with graphite monochromated Mo Kα radiation. Data were collected in a series of ϕ and ω scans in 0.50° oscillations with 10−30 s exposures, and collected and integrated using the SAINT software package.[28] Data were corrected for absorption effects using the multiscan technique (SADABS)[29] and corrected for Lorentz and polarization effects. The structures were solved using direct methods[30] and refined using the SHELXTL crystallographic software package.[31] For each structure, all non-hydrogen atoms were refined anisotropically and all hydrogen atoms were included in calculated positions but were not refined. Compounds **5b**−**d** crystallize with one-half-molecule residing on an inversion center.

Crystals of **5e** were too thin for structural determination with a standard diffractometer, so synchrotron radiation was used. Suitable crystals of **5e** were mounted on a glass fiber and the data collected at 150 K on a D8 goniostat equipped with a CCD detector at Beamline 11.3.1 at the Advanced Light Source (Lawrence Berkeley National Laboratory) using synchrotron radiation tuned to λ = 0.7749 Å. A series of 3 s data frames measured at 0.2° increments of ω were collected to calculate a unit cell. For data collection, 3 s frames were measured at 0.3° intervals of ω and ϕ. The data frames were collected using the program APEX2 and processed using the program SAINT.[28] Data were corrected for absorption effects using the multiscan technique (SADABS).[29] The structure was solved using direct methods and refined using the SHELXTL[31] crystallographic software package. Compound **5e** crystallizes with one-half molecule residing on an inversion center.

Electrochemistry. Cyclic voltammetry (CV) experiments were conducted using a potentiostat. The working electrode was either a Pt disk or an indium tin oxide (ITO) thin film on glass. The counter electrode was a Pt mesh and the reference electrode a silver wire. An internal reference, decamethylferrocene, was added to correct the measured potentials with respect to saturated calomel electrode (SCE). All experiments were carried out using a scan rate of 100 mV/s. CH_2Cl_2 used for CV experiments was purified by passing the solvent through an activated alumina tower.

Acknowledgment. We thank the Canadian Space Agency and the Natural Sciences and Engineering Research Council of Canada for funding. Samples for crystallographic analysis at the synchrotron were submitted through the SCrALS (Service Crystallography at Advanced Light Source) program. Crystallographic data were collected at the Small-Crystal Crystallography Beamline 11.3.1 at the Advanced Light Source (ALS). The ALS is supported by the U.S. Department of Energy, Office of Energy Sciences Materials Sciences Division, under contract DE-AC03-76SF00098 at Lawrence Berkeley National Laboratory.

Supporting Information Available: General experimental details, ^{1}H and ^{13}C NMR spectra, and CIF files. This material is available free of charge via the Internet at http://pubs.acs.org.

JO900590U

(28) *SAINT, Version 7.23A*; Bruker AXS Inc.: Madison, WI, 1997−2003.
(29) *SADABS, V.2.10*; Bruker AXS Inc.: Madison, WI, 2003.
(30) Altomare, A.; Cascarano, G.; Giacovazzo, C.; Guagliardi, A. *J. Appl. Crystallogr.* **1994**, *27*, 1045–1050.
(31) *SHELXTL, Version 5.1*; Bruker AXS Inc.: Madison, WI, 1997.